Taylor & Francis
Taylor & Francis Group

Structural properties of Ge nanostructured films synthesized by laser ablation

D. RIABININA*, F. ROSEI and M. CHAKER

INRS-EMT, Université du Québec,
1650 Lionel-Boulet, C.P. 1020, Varennes Qc, J3X 1S2, Canada

We compare the structural properties of nanostructured Ge films deposited by pulsed laser deposition (PLD) and crossed-beam pulsed laser deposition (CBPLD). We show that CBPLD is an excellent technique for reduction of micron-sized particles which affect the quality of nanostructured films. We demonstrate that CBPLD in the equivalent dynamic conditions of PLD yields similar nanostructured Ge films with particle sizes of $\sim$20 nm. Combining different characterization techniques we conclude that under these deposition conditions the Ge nanoparticles are amorphous.

1. Introduction

Nanostructured materials, and in particular semiconductor nanostructures [1] and thin films, may be exploited for their novel electronic and optical properties. These structures are of great interest since they have potential applications in future quantum and photonic devices [2].

Pulsed laser deposition (PLD) is a highly versatile technique for the growth of thin films and nanostructured materials. In PLD, the deposition energy can be adjusted over a wide range that makes possible the growth of dense films (e.g. to be used as waveguides) or alternatively nanocrystalline/cluster–assembled structures with excellent control over the cluster size (by depositing under a moderate pressure gas) [3, 4]. Nanostructured semiconductor films (including, e.g. Si nanostructures with remarkable photoluminescence properties) can be grown with this approach [5–10]. However, the structural properties of such nanostructures are still poorly characterized. It has been claimed that in general these nanostructures are crystalline, yet little proof has been offered [11, 12]. Often they are simply referred to as 'nanoparticles', without any structural characterization.

The lack of information on the structural properties of semiconductor nanoparticles deposited by PLD is directly related to the principle of this deposition technique. One of

---

*Corresponding author. Email: riabinina@emt.inrs.ca

the major drawbacks of PLD is the occurrence of micron-sized particulates (droplets) in the deposited films which affects film quality and limits the applicability of characterization techniques. In particular, analyses carried out by large-scale characterization techniques such as X-ray diffraction (XRD) is hindered in the presence of large crystallites, since these obscure the investigation of the morphology and overall properties of the nanostructured films.

In this work, we investigate the structural properties of cluster-assembled Ge films using an original deposition method of nanostructured droplet-free films. Recently, it has been shown that the droplet density in deposited films may be drastically reduced by using crossed-beam pulsed laser deposition (CBPLD) in vacuum [13]. CBPLD under moderate gas pressure leads to a drastic reduction of droplets, yet still yields nanostructured films. The aim of this work is to characterize the crystalline nature of the Ge clusters that compose the films.

2. Experimental details

Germanium nanostructured films were grown by both conventional PLD and by CBPLD. All Ge films were deposited at room temperature, with a film thickness of ~600 nm. (The thickness of deposited films was measured by means of a DEKTAK profilometer.) A polycrystalline Ge target (99.99%) was placed on a rotating holder inside a vacuum chamber. Radiation from a pulsed KrF laser (wavelength 248 nm, pulse duration 17 ns, repetition rate 20 Hz) was used to ablate the target. The experimental chamber was pumped down to 10^{-6} torr, then the gas flow was slowly introduced into the chamber. Laser ablation was carried out under 1 torr He background pressure. The distance between substrate and target was fixed at 50 mm. The laser density on the target was fixed at $5\,\text{J/cm}^2$. The CBPLD experimental set-up is shown in figure 1. The laser beam is separated into two beams which are focused on similar rotating Ge targets, with a laser density of $5\,\text{J/cm}^2$ for each target. The directional plasmas of the two targets were perpendicular to one another and
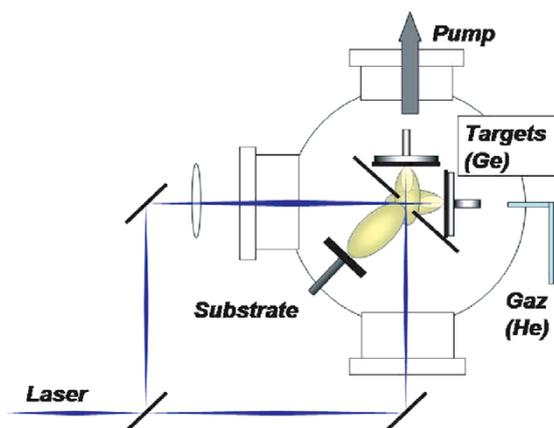

Figure 1.   Schematic diagram of the CBPLD set-up.

the distance between the targets and interaction zone was 15 mm. The interaction zone–substrate distance was fixed at 35 mm and the whole target–substrate path of the ablated material was 50 mm. Two perpendicular plasma plumes interact in a collision zone and the third resulting plume is directed toward a substrate. The diaphragm aperture width was adjusted to 1.3 cm in order to cut off the direct droplet deposition and let free the laser beam paths.

3. Results and discussion

Figure 2(a) displays a scanning electron microscopy (SEM) micrograph of a Ge film deposited by PLD. A high density of droplets (1–5 micron in diameter) is clearly visible in the image. Figure 2(b) shows an SEM image of a Ge film deposited by CBPLD.
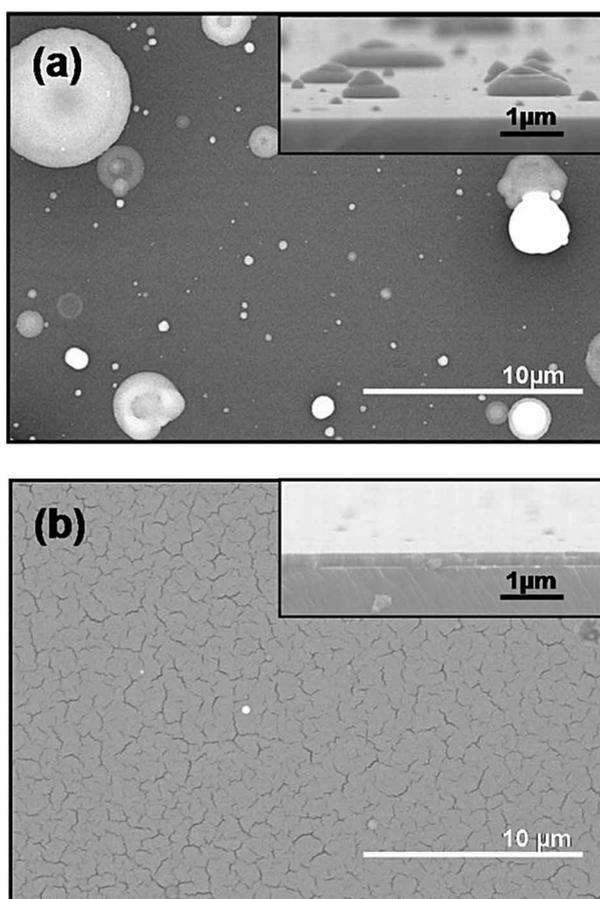

Figure 2. SEM images ($25 \times 18 \, \mu m^2$) of (a) Ge film deposited by conventional PLD (1 torr He, 5 J/cm^2, target–substrate distance 50 mm, 600 nm thickness) and (b) a droplet-free Ge film deposited by CBPLD (same experimental conditions as in (a)). The insets in (a) and (b) display cross–sectional SEM images ($5.5 \times 2.4 \, \mu m^2$).

In this micrograph, only a few droplets are visible in an area of hundreds of square microns. The insets of figures 2(a) and (b) display cross-sectional SEM images (side view). A statistical analysis reveals that the density of droplets for the film deposited by CBPLD under 1 torr He is ∼20 times lower than for the film deposited by conventional PLD.

This mechanism is rationalized as follows. The split laser beam is focused on two perpendicular (rotating) targets and creates two interacting synchronized plasma plumes. The ablated species (atoms, ions and clusters) interact in the collision zone and are deflected towards the substrate. The droplets, which are slow and heavy, traverse the interaction zone with little or no perturbation of their original trajectories. Thus, the paths of the atomic species and droplets are spatially separated. The substrate is placed along the direction of the deflected atomic species and screened from particulates by a diaphragm. Even though the diaphragm screens the particulates, some of the ablated material will reach the substrate due the eclipse effect [14], and this amounts to ∼25% of deposited material. Thus the deposited film material consists of ∼75% of the product of interaction of the plasma plumes [15].

To compare the nanoscale structure of Ge films deposited by PLD and CBPLD, we performed atomic force microscopy (AFM) measurements. Figure 3(a) shows the AFM image of Ge film deposited by PLD. A histogram of the size distribution is displayed in the inset (the average size of Ge nanoparicles is ∼20 nm). An AFM image of the Ge film deposited by CBPLD is shown in figure 3(b). The corresponding histogram is shown in the inset (the average size of the nanoparticles is ∼17 nm). The deposition conditions of both films were chosen in such a way as to conserve the deposition dynamics (the substrate–target distance was similar for PLD and CBPLD). The nanoscale structure of both films is similar. Thus, we conclude that the deposition by CBPLD enables a significant reduction of droplet density without changing film morphology at the nanoscale.

To study the crystallinity of Ge nanostructured films, the samples were analysed by XRD. In figure 4(a) and (b) we report XRD patterns of Ge films deposited by PLD and CBPLD, respectively. For both patterns, the large broad background indicates the presence of amorphous Ge. The film deposited by PLD (figure 4a) exhibits peaks which are typical of polycrystalline Ge. The peaks are very narrow with a full width at half maximum (FWHM) of the (111) diffraction peak equal to $0.2°$, which corresponds to the resolution of the diffractometer. From this, crystallite size is estimated to be larger than 50 nm. By contrast, the XRD pattern of the film grown by CBPLD (figure 4b) does not show any Ge peaks. Thus, the narrow peaks in the XRD pattern of the PLD-deposited Ge film are attributed to the droplets in the film.

We now discuss the structural nature of the Ge clusters composing the film. If these were crystalline, their typical size of 20 nm would yield broad peaks in the XRD pattern. In particular, we estimate that the (111) diffraction peak would have a FWHM of at least $0.7°$. Such a peak is clearly missing from the pattern (figure 4b), therefore we conclude that individual Ge nanoparticles are amorphous.

To confirm the amorphous nature of Ge nanoparticles deposited by PLD, we investigated Ge film by transmission electron microscopy (TEM). Figure 5 shows a TEM image of Ge film deposited by PLD under 1 torr He, 5 J/cm^2, target–substrate distance 50 mm. The image demonstrates the amorphous nature of Ge nanoparticles
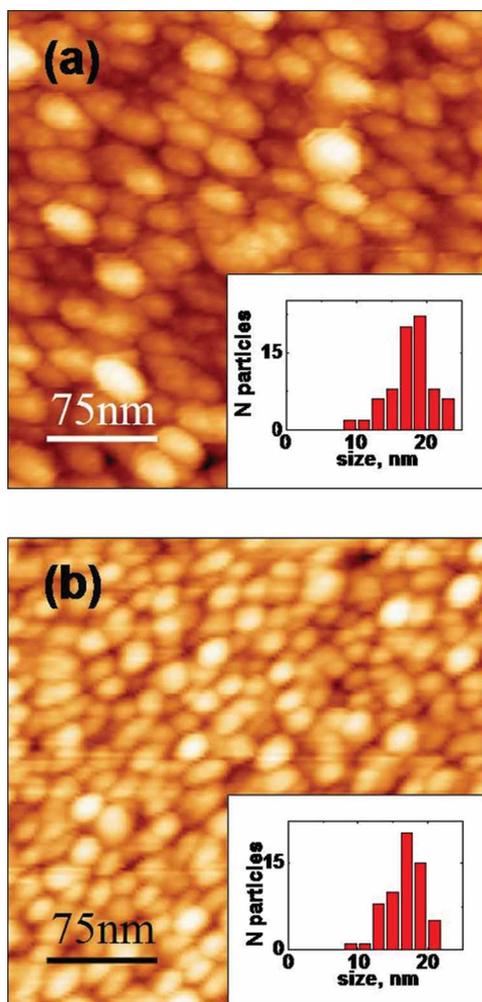
Figure 3. AFM images of Ge films (a) deposited by PLD (1 torr He, 5 J/cm^2, target–substrate distance 50 mm, 600 nm thickness), and (b) deposited by CBPLD (same experimental conditions as in figure 2b). The insets in (a) and (b) display the statistical analysis of nanoparticle size.

and thus confirms the results obtained from the XRD analysis. The average size of Ge nanoparticles characterized by TEM is equal to 14 ± 4 nm, which is much smaller than the nanoparticle size obtained by AFM analysis. We believe that TEM results are more reliable in this case because of possibility of tip convolution effects in the AFM analysis.

4. Conclusion

In conclusion, we investigated the crystallinity of Ge cluster-assembled films deposited by PLD and CBPLD under moderate gas pressure. We showed that CBPLD allows us
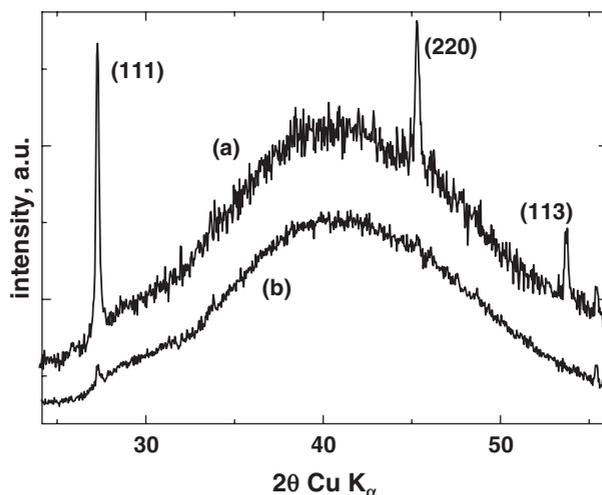
Figure 4.   X-ray diffraction patterns (a) of Ge film deposited by PLD (1 torr He, 5 J/cm^2, target–substrate distance 50 mm, 600 nm thickness), and (b) of a droplet-free film deposited by CBPLD (same experimental conditions as in figure 2b).
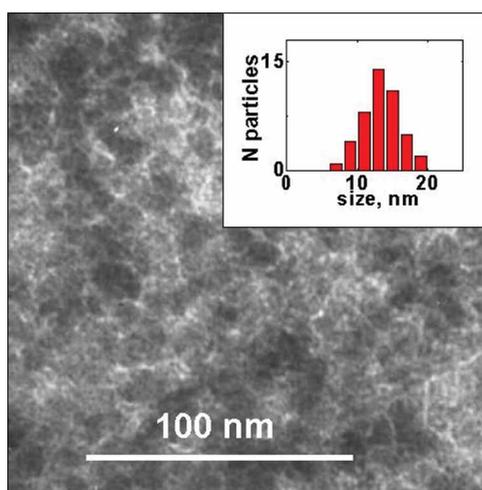

Figure 5.   TEM image of Ge film deposited by PLD (1 torr He, 5 J/cm^2, target–substrate distance 50 mm). The inset displays the statistical analysis of nanoparticle size.

to reduce drastically (by a factor of ∼20) the density of micron-sized droplets that are present in the films deposited by PLD. We also demonstrated that the nanoscale morphology of Ge films is similar for both PLD and CBPLD, and the average size of the nanoparticles does not change for analogous deposition conditions. We obtained the size of nanoparticles equal to 17 ± 4 nm by AFM and equal to 14 ± 4 nm by TEM analysis. Finally, we demonstrated that under these deposition conditions, Ge nanoparticles deposited by PLD are amorphous.

Acknowledgements

References

[1] F. Rosei. Nanostructured surfaces: challenges and frontiers in nanotechnology. J. Phys. Condens. Matter **16,** S1373 (2004).

[2] P. Lever, H. H. Tan, C. Jagadish, P. Reece, and M. Gal. Proton-irradiation-induced intermixing of InGaAs quantum dots. Appl. Phys. Lett. **82,** 2053 (2003).

[3] D. H. Lowndes, D. B. Geohegan, A. A. Puretzky, D. P. Norton, and C. M. Rouleau. Synthesis of novel thin-film materials by pulsed laser deposition. Science **273,** 898 (1996).

[4] R. Dolbec, E. Irissou, M. Chaker, D. Guay, F. Rosei, and M. A. El Khakani. Growth dynamics of pulsed laser deposited Pt nanoparticles on highly oriented pyrolitic graphite substrates. Phys. Rev. B **70,** 201406 (2004).

[5] I. A. Movtchan, R. W. Dreyfus, W. Marine, M. Sentis, M. Autric, G. Le Lay, and N. Merk. Liminescence from a Si–SiO$_2$ nanocluster-like structure prepared by laser ablation. Thin Solid Films **255,** 286 (1995).

[6] L. Patrone, D. Nelson, V. I. Safarov, M. Sentis, and W. Marine. Photoluminescence of silicon nanoclusters with reduced size dispersion produced by laser ablation. J. Appl. Phys. **87,** 3829 (2000).

[7] A. V. Kabashin, J.-P. Sylvestre, S. Patskovsky, and M. Meunier. Correlation between photoluminescence properties and morphology of laser-ablated Si/SiOx nanostructured films. J. Appl. Phys. **91,** 3248 (2002).

[8] D. B. Geohegan, A. A. Puretzky, G. Duscher, and S. J. Pennycook. Photoluminescence from gas-suspended SiOx nanoparticles synthesized by laser ablation. Appl. Phys. Lett. **73,** 438 (1998).

[9] W. Marine, L. Patrone, B. Luk'yanchik, and M. Sentis. Strategy of nanocluster and nanostructure synthesis by conventional pulsed laser ablation. Appl. Surf. Sci. **154**–**155,** 345 (2000).

[10] M. S. Tillack, D. W. Blair, and S. S. Harilal. The effect of ionization on cluster formation in laser ablation plumes. Nanotech. **15,** 390 (2004).

[11] L. Patrone, D. Nelson, V. I. Safarov, S. Giorgio, M. Sentis, and W. Marine. Synthesis and properties of Si and Ge nanoclusters produced by pulsed laser ablation. Appl. Phys. A **69,** S217 (1999).

[12] J. Levoska, M. Tyunina, and S. Leppavuori. Laser ablation deposition of silicon nanostructures. Nanostruct. Mater. **12,** 101 (1999).

[13] M. D. Stikovsky, E. B. Klyuenkov, S. V. Gapanov, J. Schubert, and C. A. Copetti. Crossed fluxes technique for pulsed laser deposition of smooth YBa2Cu3O7–*x* films and multilayers. Appl. Phys. Lett. **63,** 1146 (1993).

[14] M. Tachiki, M. Noda, K. Yamada, and T. Kobayashi. SrTiO$_3$ films epitaxially grown by eclipse pulsed laser deposition and their electrical characterization. J. Appl. Phys. **83,** 5351 (1998).

[15] E. Irissou, F. Vidal, T. Johnston, M. Chaker, and D. Guay. Influence of an inert background gas on bi-metallic cross-beam pulsed laser deposition. J. Appl. Phys. **99** (in press).